Journal of Macromolecular Science, Part A
Publication details, including instructions for authors and subscription information:
http://www.informaworld.com/smpp/title~content=t713597274

Cellulose Filter Paper with Antibacterial Activity from Surface-Initiated ATRP

Fan Tang[a]; Lifen Zhang[a]; Zhengbiao Zhang[a]; Zhenping Cheng[a]; Xiulin Zhu[a]
[a] Key Lab. of Organic Synthesis of Jiangsu Province, College of Chemistry, Chemical Engineering and Materials Science, Soochow (Suzhou) University, Suzhou, China

To cite this Article Tang, Fan , Zhang, Lifen , Zhang, Zhengbiao , Cheng, Zhenping and Zhu, Xiulin(2009) 'Cellulose Filter Paper with Antibacterial Activity from Surface-Initiated ATRP', Journal of Macromolecular Science, Part A, 46: 10, 989 — 996
To link to this Article: DOI: 10.1080/10601320903158651
URL: http://dx.doi.org/10.1080/10601320903158651

Journal of Macromolecular Science®, Part A: Pure and Applied Chemistry (2009) **46**, 989–996

ISSN: 1060-1325 print / 1520-5738 online
DOI: 10.1080/10601320903158651

Taylor & Francis
Taylor & Francis Group

Cellulose Filter Paper with Antibacterial Activity from Surface-Initiated ATRP

FAN TANG, LIFEN ZHANG, ZHENGBIAO ZHANG, ZHENPING CHENG* and XIULIN ZHU

Key Lab. of Organic Synthesis of Jiangsu Province, College of Chemistry, Chemical Engineering and Materials Science, Soochow (Suzhou) University, Suzhou, 215123, China

Received March 2009, Accepted April 2009

Poly(*tert*-butyl acrylate) (P*t*BA) bruhes were successfully grafted on the cellulose filter papers via surface-initiated atom transfer radical polymerization (ATRP). Then the grafting P*t*BA brushes were transferred into poly(acrylic acid) (PAA) in the presence of trifluoroactic acid (TFA), which can form chelate complexes with Ag^+. The Ag^+ was reduced *in situ* to obtain the silver nanoparticles decorated cellulose filter papers. Fourier transform infrared spectroscopy (FT-IR) and X-ray diffraction (XRD) were used to characterize the chemical structure of the resulting product. The morphologies of the filter paper at different stages of surface modification were investigated by field emission scanning electron microscopy (FESEM). The silver nanoparticles decorated filter paper performed good antibacterial ability against *E. coli* as compared with the original filter paper and PAA modified filter paper.

Keywords: Surface-initiated ATRP; filter paper; silver nanoparticles; antibacterial; poly(acrylic acid)

1 Introduction

Cellulose that has been widely studied for several decades (1–5) is the most abundant natural biopolymer. Structurally, it is a polymer of D-glucose in which the individual units are linked by β -glucose links from the anomeric carbon of one unit to the C-4 hydroxyl of the next unit (6). Cellulose as an abundant, inexpensive, biodegradable and renewable resource that has been many important applications because of its useful properties such as the high modulus of crystalline cellulose combined with the low weight; but for some applications, it lacks properties of synthetic polymers (7). In order to use cellulose more effectively, modifications are needed in most cases. Grafting of polymer onto the surface of cellulose is one of the widely used methods to modify cellulose. Traditionally, the grafting methods include "grafting from" and "grafting to" techniques (6–10). Using the "grafting from" technique, radicals are generated along the cellulose backbone, followed by free radical polymerization of vinyl monomers, but it is hard to predetermine the length of the graft chains from the cellulose backbone because these methods are not controlled. The grafting polymer usually has high molecular weight, broad molecular weight distribution, and the end-groups unknown (7). In most cases, the concurrent formation of homopolymers and copolymers predominates over graft copolymerization (6). As for the "grafting to" method, the polymers are pre-formed, usually by anionic or cationic polymerization, and thereafter coupled to the cellulosic backbone. However, this procedure usually yields poor grafting density and the polymerization procedures are tedious to perform (11–13).

Fortunately, living radical polymerization, especially atom transfer radical polymerization (ATRP) that introduced by Wang and Matyjaszewski (14), provides the possibility of overcoming the disadvantages of conventional free-radical polymerization. ATRP is a robust and versatile technique for its excellent controllability over the molecular weight, and polydispersity and its facility of preparation of well-defined copolymers with various architectures such as block, graft, comb, multi-armed and hyperbranched polymers (15–18). Recently, ATRP has been successfully used in the grafting modification of cellulose and it derivatives by introducing an ATRP initiator to the cellulose backbones (6, 10, 19). Carlmark et al. report the ATRP of methyl acrylate from initiators immobilized on cellulose fibers in 2002 and a block copolymer of PMA and PHEMA has been grafted from PMA-grafted cellulose fibers in 2003 (20, 21).

In recent years, materials with antibacterial properties have been paid much attention because they are used in a wide range of fields such as food packaging, sanitary

*Address correspondence to: Zhenping Cheng, Key Lab. of Organic Synthesis of Jiangsu Province, College of Chemistry, Chemical Engineering and Materials Science, Soochow (Suzhou) University, Suzhou, 215123, China. Fax: 86-512-65882787; E-mail: chengzhenping@suda.edu.cn

materials, household and medical items. Antimicrobial surfaces can be obtained by incorporating antimicrobial species either through covalent bonding or via noncovalent (via leaching) interaction to the surface (22). Much attention has been paid on utilization of the cellulose due to its good biodegradability, biocompatibility and nontoxicity. However, there are some drawbacks of the cellulose fibers because of their large surface area and ability to retain moisture, which provides an excellent environment for microorganisms to grow. In the past several years, several research efforts have attempted to modify cellulose fiber by chemically manipulating hydroxyl functionalities as anchor points for chemical derivatization. The antibacterial agents include phenols, halogens (e.g., iodine), biguanides, heavy metals (e.g., silver, tin, and mercury), phosphonium salts, and quaternary ammonium salts (22–28). Recently, several techniques, which can create antibacterial surfaces via grafting polymers with controlled polymer length and polydispersity directly from the surface using monomers containing antimicrobial groups, have been reported. Lee et al. reported that the permanent, nonleaching antibacterial paper surfaces were obtained by ATRP of 2-(dimethylamino)ethyl methacrylate and therefore, quaternization by ethyl bromide (29). Roy et al. reported the antibacterial cellulose fiber prepared via RAFT polymerization of 2-(dimethylamino)ethyl methacrylate and then quaternization by two different alkyl bromide (22).

In this work, a novel method of fabricating antibacterial filter paper using silver nanoparticles as the antibacterial agent (24–26) was developed via ATRP technique. ATRP initiators were immobilized on the filter paper surfaces first and then the surface-initiated ATRP of *tert*-butyl acrylate (*t*BA) was carried out directly. The grafting P(*t*BA) was transferred into poly(acrylic acid) (PAA) by hydrolyzation, which can form chelate complex with Ag^+. The Ag^+ can easily be reduced *in situ* to obtain the silver nanoparticles on the cellulose filter paper surfaces after a reducing agent sodium borohydride was added. The silver nanoparticles decorated filter papers performed good antibacterial ability.

2 Experimental

2.1 Materials

Cellulose filter paper was purchased from Hangzhou Xinhua Paper Co. *Ter*t-butyl acrylate (*t*BA) (99%) was supplied by Alfa Aser Co. and filtered through a basic alumina column used by removing the stabilizer before use. 2-Bromoisobutyryl bromide (98%) was supplied by Aldrich Chemical Co. and used as received. Ethyl 2-bromoisobutyrate (EBiB) (98%) was purchased from Acros and used as received. Copper (I) bromide (CuBr) (98%) and N,N,N,N',N'-pentamethyldiethyenetriamine (PMDETA) (99%) were obtained from Aldrich and used as received. Acetone (analytical reagent), tetrahydrofuran (THF, analytical reagent), and ethanol (analytical reagent) were obtained from Changshu Yangyuan Chemical Reagents Co. and the THF was remove the remainder water by reflux in the presence of sodium for 24 h.

2.2 Immobilization of Initiator on Filter Paper (Filter Paper-Br)

The preparation procedure of the initiator-modified filter paper was similar to that reported by Carlmark (20) using the hydroxyl groups on the filter paper surfaces to react with 2-bromoisobuturyl bromide. Filter paper, 2×2 cm^2, was washed with acetone and tetrahydrofuran (THF) prior to use and ultrasonicated for 5 min in both solvents. The piece of paper was immersed in a solution of 2-bromoisobuturyl bromide (5 mL, 0.04 mol), triethylamine (7 mL, 0.05 mol), and a catalytic amount of 2-dimethyl aminopyridine (DMAP) in THF (50 mL). The reaction was allowed to proceed at room temperature on a shaking device overnight. The filter paper substrate (filter paper-Br) was thereafter thoroughly washed with ethanol and THF in that order, and dried in a vacuum oven at 25°C.

2.3 Grafting PtBA with a Targeted DP of 400 on the Modified Cellulose Fibers in the Presence of a Sacrificial Initiator (Filter Paper-g-PtBA)

Surface-initiated polymerization of *t*BA was performed by ATRP, as described earlier (30). The initiator-modified paper was immersed into the reaction mixture containing *t*BA (10 mL, 0.069 mol), PMEDTA (50 μL, 0.27 mmol), Cu(I)Br (33.3 mg, 0.23 mmol), EBiB (25 μL, 0.17 mmol) and acetone (5 mL). The flask was sealed with a rubber septum and evacuated and back-filled with Ar-gas three times and then transferred into an oil bath held by a thermostat at 60°C to polymerize. After the desired polymerization time, the substrate was subjected to intense washing in THF, water, and ethanol under ultrasonic. The sample (filter paper-*g*-PtBA) was dried in vacuum at room temperature. The free polymer initiated by EBiB in the solution was collected by pouring the solution diluted with THF into a large amount of mixture solvent of methanol and water (1:1, v/v) to precipitate the P*t*BA, and then filtered and dried under vacuum until a constant weight was obtained. The graft ratio was calculated according to the following equation:

$$G\% = (W_g - W_0)/W_0 \times 100\%$$

where, W_g and W_0 are weights of grafted cellulose filter paper and original cellulose filter paper, respectively.

2.4 Hydrolysis of Grafting PtBA (Filter Paper-g-PAA) and PtBA in Bulk

The filter paper grafted with PtBA was placed into a flask, which contained a mixture of 3 mL of trifluoroacetic acid

(TFA) and 20 mL of dichloromethane (31). The Hydrolysis reaction was performed for 24 h. Then, the filter paper was subjected to intense washing with acetone, water, and ethanol under ultrasonic. Afterwards, the cellulose grafted with PAA (filter paper-*g*-PAA) was dried under reduced pressure at room temperature. The procedure of hydrolysis of PtBA in bulk was similar to the above. After accomplishment of the hydrolysis reaction, excess reagents (20 mL) was removed by rotatory evaporation and dried under vacuum for 24 h. Then the obtained white powder was dissolved in THF and poured into an excess of hexane to precipitate PAA and then filtered and dried under vacuum.

2.5 Preparation of Silver Nanoparticles Decorated Filter Paper (Filter Paper-g-PAA/Ag)

The plentiful carboxyl groups in poly(acrylic acid) (PAA) can form a chelate complex with Ag^+ (32), giving rise to cellulose fiber/nanosilver particle hybrid composites. The filter paper covered with PAA was immersed into a 25 mL flask charged with 20 mL of $AgNO_3$ aqueous solution (0.04 M), and the flask was shaken overnight in the dark. After the filter paper had washed with distilled water five times, it was immersed into a flask containing 20 mL of distilled water; and then 8 mL of $NaBH_4$ solution (0.1 M) was added dropwise under shaking. The Ag^+ was reduced by $NaBH_4$ *in situ* and silver nanoparticles were formed on the surfaces of the filter paper (filter paper-*g*-PAA/Ag).

2.6 Antibacterial Assessment

Antibacterial activity of the silver nanoparticles decorated filter paper was evaluated by optical density method described as reported (33). A representative bacteria colony was picked off, placed in a LB broth and incubated at 37°C for 24 h. Then the obtained fresh culture, where bacteria cells grew luxuriantly, was ready for an antibacterial test. 50 μL of the fresh culture was inoculated into the LB broth medium (5 mL) containing filter papers covered with PAA and decorated with silver nanoparticles, respectively, and the mixtures were shaken in a shaking bed for 29 h. During incubation, turbidity of the medium was measured at 600 nm 9 times with a spectrophotometer.

2.7 Characterizations

The molecular weights and molecular weight distributions (M_w/M_n) of the polymers were determined with a Waters 1515 gel permeation chromatograph equipped with a refractive-index detector, with HR1, HR3, and HR4 columns with molecular weight range 100–500,000 calibrated with poly(methyl methacrylate) standard samples. THF was used as the eluent at a flow rate of 1.0 mL/min and operated at 30°C. FT-IR spectra were measured using a Varian Scimiter 1000 with the sample dispersed in KBr pellets. The thermal stability was determined with a TA 2010 thermogravimetric analyzer at a heating rate of 20°C/min in nitrogen. Field emission scanning electron microscopy (FESEM) images were recorded on a JEOL JSM-6700F FESEM at an accelerating voltage of 5 kV. The metal ion concentrations were determined by Varian SpectrAA-220FS. The optical density (OD) of the medium was measured with a spectrophotometer (721 MC UV-Vis, Shanghai, China).

3 Results and Discussion

3.1 Surface-initiated ATRP of tBA on Filter Paper Modified with ATRP Initiator

Filter paper was chosen as the cellulose fiber substrate due to its wide application in our daily lives and its low cost. In order to obtain the antibacterial filter paper surfaces, a five-step modification method via surface-initiated ATRP was demonstrated as shown in Scheme 1. The key step is the immobilization of ATRP initiators on the surfaces of the filter paper. In this work, the initiator-functionalized filter paper was obtained by the reaction between the hydroxyl groups on the surface of cellulose fibers and 2-bromoisobuturyl bromide, which yielded bromo-ester groups known as efficient initiators for ATRP on the substrate surfaces.

Surface-initiated ATRPs of tBA were carried out on the surfaces of the initiator-functionalized filter papers. Cu(I)Br and the ligand PMEDTA served as catalysts in the ATRP reaction, and acetone was used as the solvent. Adding sacrificial initiators to a ATRP reaction system is a common method to control the length of the grafts from surface confined initiators (21). In this work, EBiB as a sacrificial initiator was also added so that the molecular weight of the grafting polymer could be well-tailored. Since EBiB initiates polymerization of tBA in solution, a bulk polymer was formed simultaneously as the surface grafting. Analysis of the bulk polymer gives an idea of the molecular weight and polydispersity of the grafted polymer, even though the kinetics of the surface polymerization may differ somewhat from that of the bulk (21).

A series of cellulose-*g*-PtBA copolymers were prepared using surface-initiated ATRP. The graft ratio of P*t*BA on the cellulose fiber was calculated by gravimetric analysis. To ensure complete removal of physically adsorbing, or loosely attaching homopolymers, the samples were repeatedly washed with THF and acetone. The weight gain of filter paper-*g*-P*t*BA copolymers was then compared with filter paper-Br. As can be seen from Table 1, the molecular weight in the bulk increased from 14500 g/mol to 32500 g/mol with the polymerization time increasing from 2 h to 14 h and the M_w/M_n values were low (from 1.1 $\sim$ 1.3) except the sample cellulose-g-PtBA-2. The reason for the sample of cellulose-g-PtBA-2 was somewhat uncontrollable maybe that a rapid dynamic equilibrium between growing radicals and dormant species wasn't established and kept a

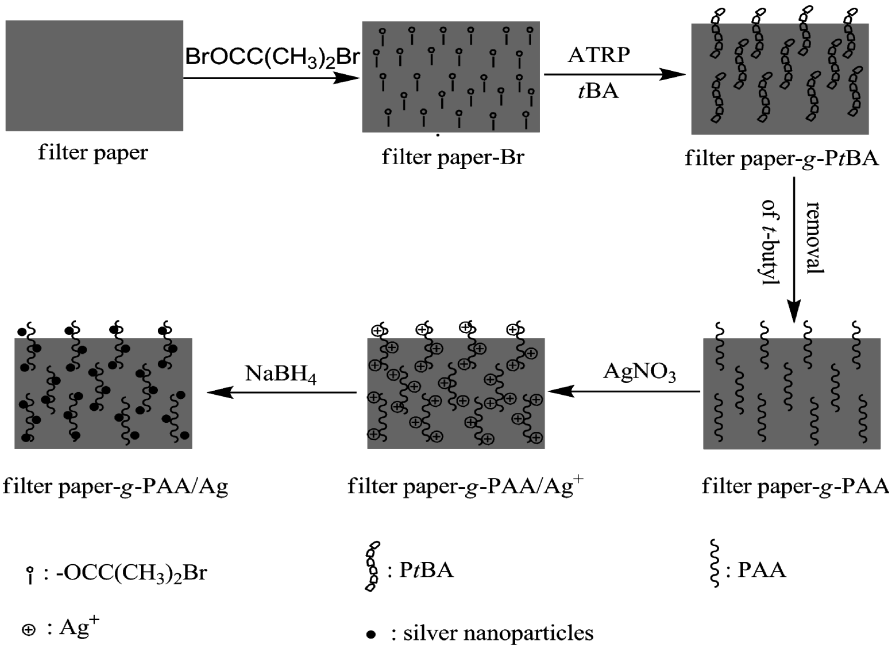

Sch. 1. Schematic diagram illustrating the modification of the cellulose filter paper by surface-initiated ATRP.

relatively high concentration of radicals at the beginning of polymerization. The graft ratio was investigated at the same time, as listed in Table 1. It can be seen that the graft ratio also increased with the polymerization time (up to 32%). All these results indicate that the polymerization of P*t*BA can be well-controlled under the present polymerization conditions.

3.2 Hydrolysis of Grafting PtBA on the Filter Paper and PtBA in Bulk

The ester groups of P*t*BA can easily be hydrolyzed into carboxyl groups by TFA in CH_2Cl_2 just at room temperature. The plentiful carboxyl groups in PAA can be used for chelating Ag^+, giving rise to filter paper-*g*-PAA/Ag hybrid composites after the Ag^+ was converted to Ag nanoparticles by $NaBH_4$ *in situ*. This method using the grafted PAA chains to sequester Ag^+ has some advantages compared with the methods of cellulose derivatives as templates to adsorb metal ions, such as: (i) there are more carboxyl groups than the small molecular carboxyl in the original filter paper; (ii) the metal ion content can be controlled by the grafting polymer density and the length of grating polymer; (iii) the metal-loaded cellulose are relatively stable due to the protective nature of the polymer overlayer; and (iv) hybrid polymer/metal nanocomposites can be readily obtained (32). From Table 1, it can be seen that the content of the silver nanoparticles on the surfaces of the functionalized filter paper can be easily adjusted from 0.22 mg/cm^2 to 0.43 mg/cm^2 by just controlling the surface-initiated ATRP polymerization time from 2 h to 14 h, fully demonstrating the advantage of this method.

3.3 Analysis by FT-IR

Figure 1 shows the FT-IR spectra of the original filter paper, filter paper-Br, filter paper-*g*-P*t*BA and filter paper-*g*-PAA. As can be seen from Figure 1a, a broad band at 3420 cm^{-1} is attributed to hydroxyl groups and the absorption bands

Table 1. The data of molecular weight, polydispersity, grafting ratio and Ag content with different polymerization time

Sample	*Grafting time (h)*	*M_n in bulk*	*M_w/M_n*	*Grafting ratio (%)*	*Ag content[a] (mg/cm^2)*
cellulose-g-P*t*BA-2	2	14500	1.6	12	0.22
cellulose-g-P*t*BA-4	4	20700	1.3	18	0.29
cellulose-g-P*t*BA-14	14	32500	1.1	32	0.43

[a]Ag content was calculated by the equation: $C_{Ag} = C_{AAS} \times V/A$, where C_{Ag}, C_{AAS}, V, and A are the Ag content, the Ag concentration measured by atomic absorption spectrometry (AAS), the whole volume of the $AgNO_3$ aqueous solution and the area of the filter papers, respectively.

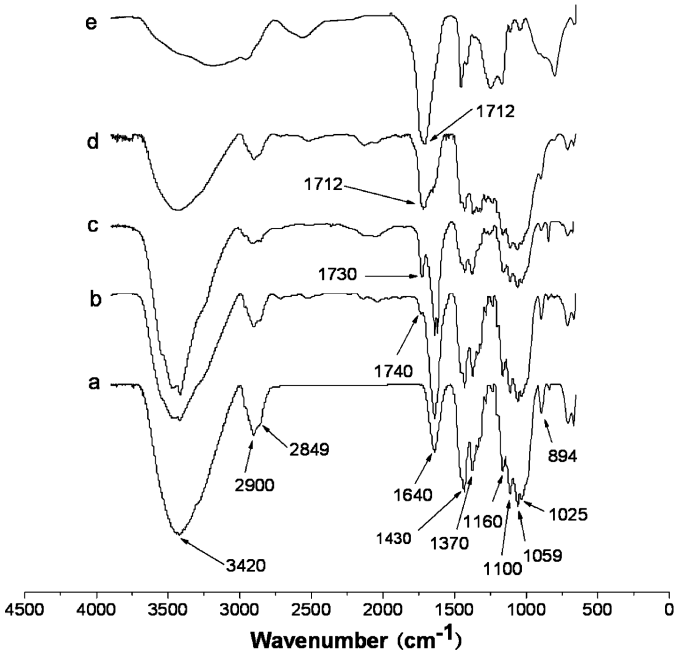

Fig. 1. FT-IR spectra of the original filter paper (a), filter paper-Br (b), filter paper-*g*-P*t*BA (c), filter paper-*g*-PAA (d) and PAA hydrolyzed from PtBA in bulk (e).

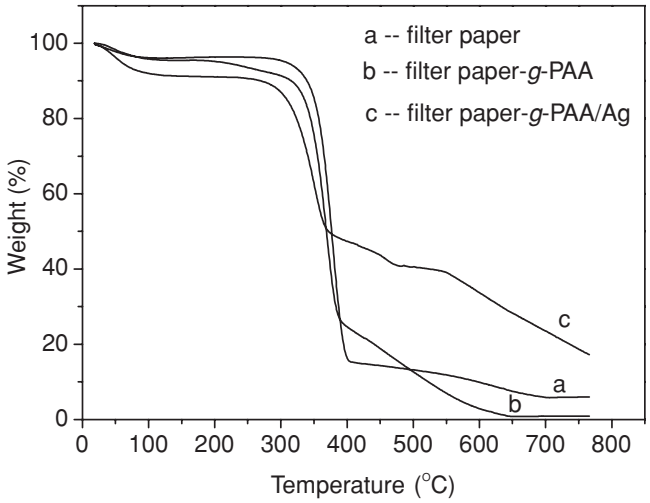

Fig. 2. TGA thermograms of the original filter paper (a), filter paper-*g*-PAA (b) and the filter paper-g-PAA/Ag (c) for the sample after polymerization of *t*BA for 14 h.

at 2900 and 2849 cm^{-1} are characteristic of C-H linkages. The peak at 2849 cm^{-1} is assigned to asymmetric and symmetric stretching vibrations resulting from CH_2 bonds. The peak at 1640 cm^{-1} is assigned to the stretching absorption resulting from H-O-H intermolecular linkages, and there are two absorption bands around 1430 and 1370 cm^{-1} due to C-H symmetric bending from CH_2 and C-H bending, respectively. The weak bands at 1059 and 1025 cm^{-1} are attributed to skeletal vibrations involving C-O stretching. Other peaks at 1160 cm^{-1}, 1100 cm^{-1} and 894 cm^{-1}, attributable to asymmetric bridge C-O-C stretching and C-H deformation, respectively, are characteristic of amorphous cellulose (34). A new peak at 1740 cm^{-1} appeared in cellulose-Br in Figure 1b, which can be assigned to carbonyl group (21, 35, 36), indicating the 2-bomoisobutyrates had successfully been immobilized on the surfaces of the cellulose fiber. After grafting polymerization of P*t*BA on the cellulose surface, the appearance of a new medium intense peak at 1730 cm^{-1} in Figure 1c is attributable to the ester group (-COO-) (30, 31, 37), suggesting that the successful grafting of the P*t*BA brushes on the filter paper surface. The FT-IR spectrum for the filter paper-*g*-PAA is shown in Figure 1d. The peak at 1730 cm^{-1} disappeared and a new peak at 1712 cm^{-1} which is usually representative of PAA appeared and it is consistent with the PAA hydrolyzed from PtBA in bulk shown in Figure 1e (30, 31, 37), indicating that the P*t*BA was successfully transferred into PAA by hydrolysis. There is also a decrease in the absorption at the band localized at 1640 mcm^{-1} (stretching H-O-H) due to a decrease in the H-O-H interactions because of the presence of the PAA chains.

3.4 TGA Analysis

Thermogravimetric (TGA) analysis was used to study the decomposition pattern and the thermal stability of the grafted cellulosic copolymers. Figure 2 displays the TGA weight loss curves for some samples of the original filter paper, filter paper-*g*-PAA, and the filter paper-*g*-PAA/Ag. As seen in Figure 2a, the original filter paper decomposed in the range of 290–405°C and about 13.5 wt% of sample remaining at 500°C, as observed by previous works (7, 9, 38). The decomposition of filter paper-*g*-PAA shows a two-step-degradation profile, with the first degradation step due to cellulose and then PAA grafts, and only yields a small amount of residual mass (0.83 wt%) as shown in Figure 2b due to the PAA grafted on the filter paper surfaces (39, 40). There is more residual mass for the sample of filter paper-*g*-PAA/Ag hybrid composites below 760°C, shown in Figure 2c as compared with the sample of filter paper-*g*-PAA due to the presence of the silver nanoparticles on the surface of the filter paper (32).

3.5 XRD Analysis

X-ray diffraction (XRD) was used to examine the crystal structure of the sample of filter paper-*g*-PAA/Ag hybrid composites as shown in Figure 3. The XRD peaks appearing at $2\theta = 37.9°$, 44.2°, and 64.3° correspond to the (111), (200), and (220) planes of the face-centered-cubic (fcc) silver, respectively, indicating that silver nanoparticles formed in the brushes are high crystallinity (41, 42). These data are in good agreement with the data in the Powder Diffraction

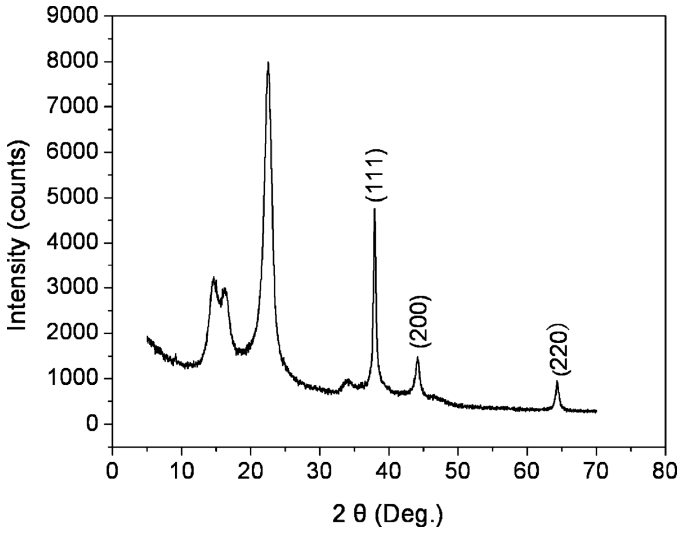

Fig. 3. XRD pattern of the filter paper-*g*-PAA/Ag hybrid composites for the sample after polymerization of *t*BA for 14 h. Ticks indicate reference peaks for *fcc*-silver (PDF-No. 00-004-0783).

File (PDF-No.: 00-004-0783). No diffraction peaks corresponding to silver oxide are observed, which confirms that the silver nanoparticles stabilized by PAA brushes on the surfaces of the filter paper are successfully formed.

3.6 Morphology Analyzed by FESEM

Figure 4 shows the morphologies of the original filter paper, filter paper-*g*-PAA and filter paper-*g*-PAA/Ag from FESEM. From Figure 4c, a lot of particles, attributable to the silver nanoparticles formed *in situ*, can be seen on the surface of the surface-modified filter paper as compared with the original filter paper (Figure 4a) and filter paper-*g*-PAA (Figure 4b), suggesting the successful synthesis of silver nanoparticles on the filter paper. The components of the resulting filter paper-*g*-PAA/Ag hybrid composites were measured using an FESEM instrument equipped with an energy dispersive spectrometer (EDS) analyzer. EDS analysis confirmed a higher silver content on the surface of the filter paper as seen in Figure 4d (32). In addition, from

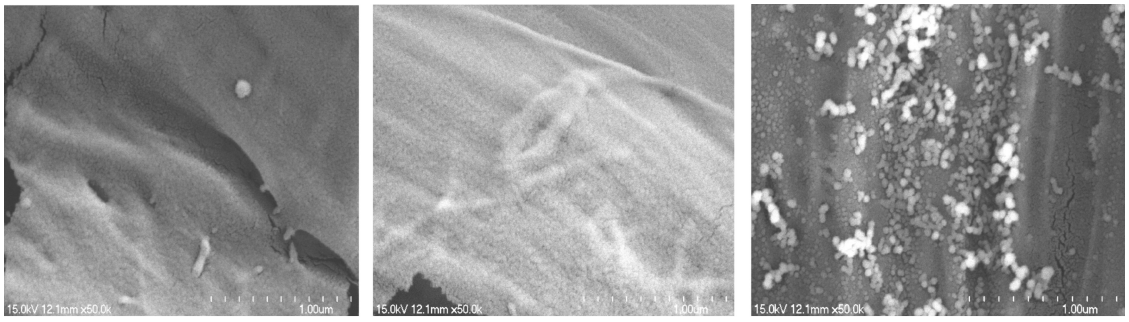

(a) (b) (c)

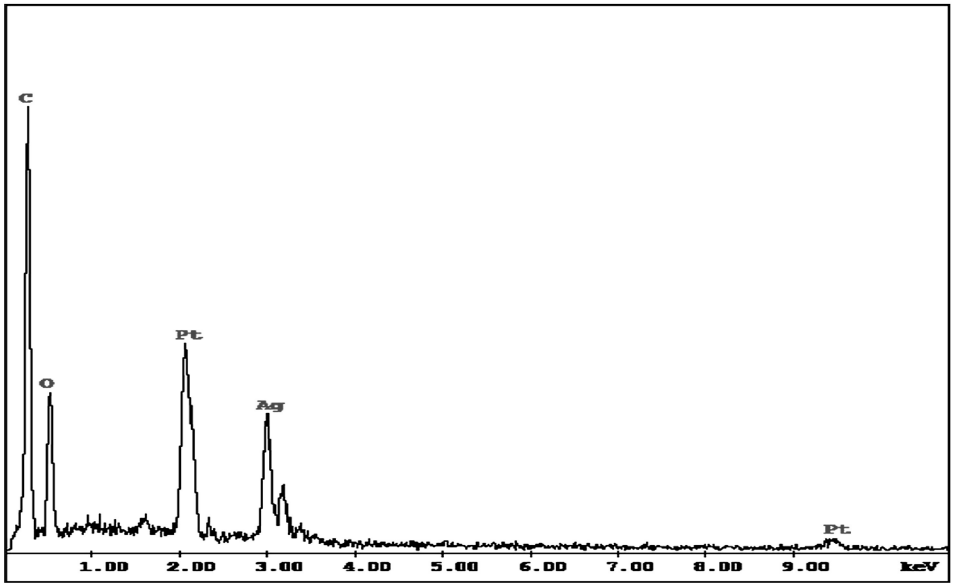

(d)

Fig. 4. FESEM images of the original filter paper (a), filter paper-*g*-PAA (b) and filter paper-*g*-PAA/Ag (c); and EDS spectrum of the filter paper-*g*-PAA/Ag (d).

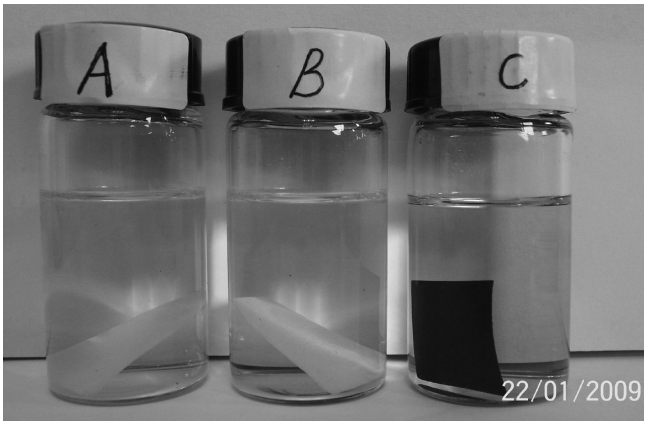

Fig. 5. Photos of the original filter paper (A), filter paper-*g*-PAA (B), and filter paper-*g*-PAA/Ag (C) in water.

Figure 5, it can be seen that the filter paper turns black after the decoration by silver nanoparticles on the surface (Figure 5C), while the original filter paper (Figure 5A) and the filter paper-*g*-PAA (Figure 5B) are white.

3.7 Antibacterial Assessment

The ability of the silver decorated filter paper to inhabit bacteria was tested according to the reported method by Li et al. (33), and the results are described in Figure 6. The optical density (OD) of the medium will change with the bacterial cell propagating due to that the bacterial cell is opaque. *E. coli* was selected to the bacterial cell and four controls in which there is no presence of filter paper (a), the presence of the original filter paper (b), the presence of the filter paper-*g*-PAA (c) and the filter paper-*g*-PAA/Ag (d) were conducted. From Figure 6, it can be seen that both the original filter paper (b) and filter paper-*g*-PAA (c) perform no antibacterial activity because the OD was almost the same as that of the control of no filter existence (a). However, after surface functionalization by silver nanoparticles the filter paper-*g*-PAA/Ag exhibits good antibacterial activity as compared with the original filter paper and the filter paper-*g*-PAA.

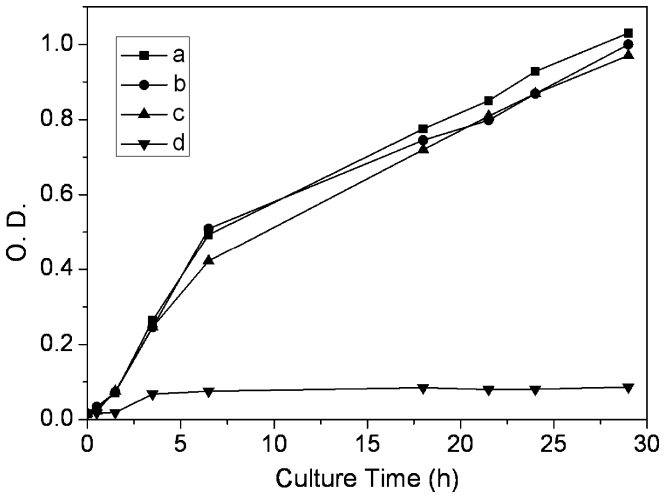

Fig. 6. OD vs. culture time of the medium (a), original filter paper (b), filter paper-*g*-PAA (c), and filter paper-*g*-PAA/Ag (d).

4 Conclusions

A novel method of fabricating antibacterial filter paper using silver nanoparticles as the antibacterial agent was demonstrated via surface-initiated ATRP technique. The process involved (i) immobilization of initiators on the filter paper surfaces, (ii) modification of the filter paper surfaces via covalent bonding of well-defined PtBA brushes from surface-initiated ATRP of tBA, (iii) transferring the grafting PtBA into PAA by hydrolyzation in the presence of TFA, and (iv) chelating Ag^+ into the PAA brushes and subsequently reducing it into silver nanoparticles *in situ* by a reducing agent sodium borohydride. The silver nanoparticles decorated filter papers were endowed with good antibacterial ability against *E. coli* compared with the original filter paper and PAA grafting filter paper.

Acknowledgments

The financial support of this work by the National Natural Science Foundation of China (Nos.20874069 and 50803044), the Science and Technology Development Planning of Jiangsu Province (Nos. BK2007702 and BK2007048), the International Cooperation Foundation of Jiangsu Province (No. BZ2007037), the Pre-research Project of Soochow University, Program of Innovative Research Team of Suzhou University and Qing Lan Project are gratefully acknowledged.

References

1. Yasuda, I.H., Wray, J.A. and Stannett, V. (1963) *J. Polym. Sci. Part. C,* 387–402.
2. Heinze, T. and Liebert, T. (2001) *Prog. Polym. Sci.*, 26, 1689–762.
3. Klemm, D., Heublein, B., Fink, H.P. and Bohn, A. (2005) *Angew. Chem. Int. Ed.*, 44, 3358–93.
4. Shi, H.Y., Zhang, L.M., Ma, Y.Q. and Yi, J.Z. (2007) *J. Macromol. Sci., Part A: Pure & Appl. Chem.,* 44, 1109–13.
5. Huang, X.S. and Netravali, N. (2008) *J. Macromol. Sci., Part A: Pure & Appl. Chem.*, 45, 899–906.
6. Shen, D.W., Yu, H. and Huang, Y. (2005) *J. Polym. Sci., Part A: Polym. Chem.*, 43, 4099–108.
7. Lindqvist, J. and Malmström, E. (2006) *J. Appl. Polym. Sci.*, 100, 4155–62.
8. Kang, H.L., Liu, W.Y., Liu, R.G. and Huang, Y. (2008) *Macromol. Chem. Phys.*, 209, 424–30.

9. Barsbay, M., Gven, O., Martina, H.S. and Thomas, P.D. (2007) *Macromolecules*, 40, 7140–7.
10. Ifuku, S. and John, F.K. (2008) *Biomacromolecules*, 9, 3308–13.
11. Biermann, C.J., Chung, J.B. and Narayan, R. (1987) *Macromolecules*, 20, 954–7.
12. Mansson, P. and Westfeldt, L. (1981) *J. Polym. Sci. Part A: Polym. Chem.*, 19, 1509–15.
13. Tsubokawa, N., Iida, T. and Takayama, T. (2000) *J. Appl. Polym .Sci.*, 75, 515–22.
14. Wang, J.S. and Matyjaszewski, K. (1995) *Macromolecules*, 28, 7901–10.
15. Wang, J.S. and Matyjaszewski, K. (1995) *J. Am. Chem. Soc.*, 117, 5614–15.
16. Patten, T.E. and Matyjaszewski, K. (1998) *Adv. Mater.*, 10, 901–15.
17. Shipp, D.A., Wang, J.L. and Matyjaszewski, K. (1998) *Macromolecules*, 31, 8005–8.
18. Cheng, Z.P., Zhu, X.L., Shi, Z.L., Neoh, K.G. and Kang, E.T. (2005) *Ind. Eng. Chem. Res.*, 44, 7098–104.
19. Stmark, E., Harrisson, S. and Malmstrm, E. (2007) *Biomacromolecules*, 8, 1138–48.
20. Carlmark, A. and Malmstrom, E. (2002) *J. Am. Chem. Soc*, 124, 900–1.
21. Carlmark, A. and Malmstrom, E. (2003) *Biomacromolecules*, 4, 1740–5.
22. Roy, D., Knapp, J.S., Guthrie, J.T. and Perrier, S. (2008) *Biomacromolecules*, 9, 91–9.
23. Son, W.K., Youk, J.H., Lee, T.S. and Park, W.H. (2004) *Macromol. Rapid Commun.*, 25, 1632–7.
24. Son, W.K., Youk, J.H. and Park, W.H. (2006) *Carbohyd. Polym.*, 65, 430–4.
25. Kulpinski, P. (2007) *e-polymer*s, No. 068.
26. Lee, H.J., Yeo, Y. and Jeong, S.H. (2003) *J. Mater. Sci.*, 38, 2199–204.
27. Luong, N.D., Lee, Y.K. and Nama, J.D. (2008) *Eur. Polym. J.*, 44, 3116–21.
28. Adamopoulos, L., Montegna, J. and Hampikian, G. (2007) *Carbohyd. Polym.*, 69, 805.
29. Lee, S.B., Koepsel, R.R., Morley, S.W., Matyjaszewski, K., Sun, Y.J. and Russell, A.J. (2004) *Biomacromolecules*, 5, 877–82.
30. Wu, T., Gong, P., Szleifer, I., Vlcek, P., Sÿubr, V. and Genzer, J. (2007) *Macromolecules*, 40, 8756–64.
31. Liu, C., Wang, G. W., Zhang, Y. and Huang, J.L. (2008) *J. Appl. Polym. Sci.*, 108, 777–84.
32. Pei, X.W., Hao, J.C. and Liu, W.M. (2007) *J. Phys. Chem. C*, 111, 2947–52.
33. Li, Z., Zhuang, X.P., Guan,Y.L. and Yao, K.D. (2002) *Polymer*, 43, 1541–7.
34. LoríA-bastarrachea, M.I., Carrillo-Escalante, H.J. and Aguilar-vega, M.J. (2002) *J. Appl. Polym. Sci.*, 83, 386–93.
35. Ohno, K., Morinaga, T., Koh, K., Tsujii, Y. and Fukuda, T. (2005) *Macromolecules***,** 38, 2137–42.
36. Liu, D.M., Chen, Y.W., Zhang, N. and He, X.H. (2006) *J. Appl. Polym. Sci.*, 101, 3704–12.
37. Qin, S.H., Saget, J., Pyun, J., Jia, S. and Kowalewski, T. (2003) *Macromolecules*, 36, 8969–77.
38. Roy, D., Guthrie, J.T. and Perrier, S. (2005) *Macromolecules*, 38, 10363–72.
39. Hojjati, B., Sui, R. and Charpentier, P.A. (2007) *Polymer*, 48, 5850–8.
40. Li, D.J., Sheng, X. and Zhao, B. (2005) *J. Am. Chem. Soc.*, 127, 6248–56.
41. Lu, Y., Mei, Y., Schrinner, M., Möller, M.W. and Breu, J. (2007) *J. Phys. Chem. C*, 111, 7676–81.
42. Cheng, D., Zhou, X., Xia, H. and Chan, H.S.O. (2005) *Chem. Mater.*, 17, 3578–81.